Conclusions

This study presents a quantitative physicochemical analysis of the aqueous chemistry of the Cp_2MCl_2 compounds (M = Ti, V, Zr). The chloride hydrolysis of these compounds has been shown to be both more rapid and more extensive than that of the reference compound for this study, cisplatin, although the data obtained from both classes of compounds can be analyzed with essentially the same equilibrium model. A key difference between the hydrolysis behavior of these two classes of compounds is that for the Cp_2MCl_2 complexes, another concurrent process, namely loss of cyclopentadienide, can become important depending upon the nature of M and the solution pH. In the case where M = Ti, ring loss is extensive at physiological pH, while it is not observed with Cp_2VCl_2. Since both of these compounds are antitumor active, any discussion of their mechanism of action must take this observation into account. It is suggested that, because of the structural integrity of the Cp_2V^{2+} framework under physiological conditions, Cp_2VCl_2 should be the compound of choice for any future studies involving Cp_2MCl_2-biomolecule interactions.

Acknowledgment. We are grateful to National Science Foundation (CHE8306255) and to Sigma Xi (Grant-in-Aid award to J.H.T.) for support of this research. We also thank Dr. Paul J. Toscano for assistance in recording the CPMAS ^{13}C NMR spectrum of **1**, Ray Wieboldt for assistance in developing the methodology for H_2O solvent suppression in the ^1H NMR experiments, and Scott W. Campbell for assistance in the numerical analyses.

Registry No. $Cp_2Ti(H_2O)_2^{2+}$, 75576-50-0; $Cp_2V(H_2O)_2^{2+}$, 93895-89-7; Cp_2TiCl_2, 1271-19-8; Cp_2VCl_2, 12083-48-6; Cp_2ZrCl_2, 1291-32-3.

Metastable Fe/S Clusters. The Synthesis, Electronic Structure, and Transformations of the $[Fe_6S_6(L)_6]^{3-}$ Clusters (L = Cl^-, Br^-, I^-, RS^-, RO^-) and the Structure of $[(C_2H_5)_4N]_3[Fe_6S_6Cl_6]$

M. G. Kanatzidis, W. R. Hagen, W. R. Dunham, R. K. Lester, and D. Coucouvanis*

Contribution from the Department of Chemistry, University of Michigan, Ann Arbor, Michigan 48109. *Received August 20, 1984*

Abstract: A series of new novel $[Fe_6S_6(L)_6]^{3-}$ clusters (L = Cl, Br, I, SC_6H_4-*p*-CH_3, OC_6H_4-*p*-CH_3) have been synthesized and characterized as their Et_4N^+ salts. The crystal structure of $(Et_4N)_3Fe_6S_6Cl_6 \cdot CH_3CN$ (I) is described in detail. The latter crystallizes in the $C2/c$ space group with cell constants a = 20.092 (5) Å, b = 17.937 (6) Å, c = 13.790 (4) Å, β = 91.33 (2)°, Z = 4, and V = 4968 Å^3. The structure was solved by conventional methods from 2604 reflections and was refined by full-matrix least-squares techniques (206 parameters) to a final R value of 0.047. The anion in I contains the new $[Fe_6S_6]^{3+}$ distorted hexagonal prismatic core which consists of alternating tetrahedral Fe and triply bridging S atoms. Three of the Fe coordination sites are occupied by core sulfide atoms while the fourth coordination site is filled by the terminal chloride ligands. There are two sets of Fe···Fe distances and Fe–S–Fe angles in the Fe_6S_6 core with mean values of 2.765 (3) Å, 3.790 (8) Å and 74.7 (1)°, 113.2 (3)°, respectively. The $[Fe_6S_6]^{3+}$ core appears to be a metastable entity and is easily transformed, upon heating, to the thermodynamically more stable $[Fe_4S_4]^{2+}$ core. The chemical properties and electronic spectra of these clusters are reported. The clusters in CH_2Cl_2 solution display a reversible 3−/2− couple and an irreversible 3−/4− couple. Zero field and magnetically perturbed Mössbauer spectra are reported for all clusters. Their isomer shift and quadrupole splitting values are quite similar to those in the corresponding $(Fe_4S_4(L)_4)^{2-}$ cubane clusters. The $(Fe_6S_6(L)_6)^{3-}$ prismane clusters exhibit characteristic electron paramagnetic resonance (EPR) spectra (9 K) indicative of $S = {}^1/_2$ ground states. The Mössbauer and EPR results, in conjunction with magnetic susceptibility data in the 1.5–300 K temperature range for I, also are consistent with an $S = {}^1/_2$ ground state. The biological implications of the $[Fe_6S_6]$ cores are discussed.

Synthetic analogues for the $(Fe_4S_4(Cys)_4)^{2-,3-}$, $(Fe_2S_2(Cys)_4)^{2-}$, and $(Fe(Cys)_4)^{2-,1-}$ active sites in the non-heme iron proteins (NHIP) have been synthesized and structurally characterized.[1-3] The analogue complexes contain aliphatic or aromatic thiolate terminal ligands in place of the cysteinyl residues, and their syntheses can be accomplished by various procedures. The "spontaneous self-assembly" synthesis[4] of the $(Fe_4S_4(SR)_4)^{2-}$ and $(Fe_2S_2(SR)_4)^{2-}$ clusters from mixtures of appropriate reactants occurs readily and its success is based on the premise that "... clusters derived from substitutionally labile iron(II,III) reactants form as a consequence of being the thermodynamically most stable, soluble reaction products".[4]

More recently spontaneous self-assembly reactions have been employed successfully in the synthesis of interesting clusters with less direct biological relevance which include the $(Fe_6S_9(SR)_2)^{4-}$,[5] $(Fe_3S_4(SR)_4)^{3-}$,[6] and $(Fe_6(S)_8(PEt_3)_6)^{2+}$[7] ions. In these complex

(1) (a) Averill, B. A.; Herskovitz, T.; Ibers, J. A.; Holm, R. H. *J. Am. Chem. Soc.* **1973**, *95*, 3523–3534. (b) Hagen, K. A.; Reynolds, J. G.; Holm, R. H. *J. Am. Chem. Soc.* **1981**, *103*, 4054–4063. (c) Christou, G.; Garner, C. D. *J. Chem. Soc., Dalton Trans.* **1979**, 1093–1094.

(2) (a) Mayerle, J. J.; Denmark, S. E.; DePamphilis, B. V.; Ibers, J. A.; Holm, R. H. *J. Am. Chem. Soc.* **1975**, *97*, 1032. (b) Coucouvanis, D.; Swenson, D.; Stremple, P.; Baenziger, N. C. *J. Am. Chem. Soc.* **1979**, *101*, 3392–3394.

(3) (a) Holah, D. G.; Coucouvanis, D. *J. Am. Chem. Soc.* **1975**, *97*, 6917–6919. (b) Lane, R. W.; Ibers, J. A.; Frankel, R. B.; Holm, R. H. *Proc. Natl. Acad. Sci. U.S.A.* **1975**, *72*, 2868–2872. (c) Coucouvanis, D.; Swenson, D.; Baenziger, N. C.; Murphy, C.; Holah, D. G.; Sfarnas, N.; Simopoulos, A.; Kostikas, A. *J. Am. Chem. Soc.* **1981**, *103*, 3350–3362. (d) Koch, S. A.; Millar, M. *J. Am. Chem. Soc.* **1982**, *104*, 5255. (e) Millar, M.; Lee, J.; Koch, S. A.; Fikar, R. *Inorg. Chem.* **1982**, *21*, 4105.

(4) Holm, R. H. *Chem. Soc. Rev.* **1981**, *10*, 455–490.

(5) (a) Christou, G.; Holm, R. H.; Sabat, M.; Ibers, J. A. *J. Am. Chem. Soc.* **1981**, *103*, 6269–6271. (b) Christou, G.; Sabat, M.; Ibers, J. A.; Holm, R. H. *Inorg. Chem.* **1982**, *21*, 3518–3526. (c) Henkel, G.; Tremel, W.; Krebs, B. *Angew. Chem., Int. Ed. Engl.* **1981**, *20*, 1033–1034.

(6) (a) Hagen, K. S.; Holm, R. H. *J. Am. Chem. Soc.* **1982**, *104*, 5496–5497. (b) Hagen, K. S.; Holm, R. H. *Inorg. Chem.* **1984**, *23*, 418–427.

0002-7863/85/1507-0953$01.50/0 © 1985 American Chemical Society

ions the structures of the $[Fe_6(\mu\text{-}S)_6(\mu_3\text{-}S)_2(\mu_4\text{-}S)]^{2-}$, $[Fe_3(\mu\text{-}S)_4]^{+}$, and $[Fe_6(\mu_3\text{-}S)_8]^{2+}$ cores, respectively, have been established by X-ray crystallography.

The spontaneous self-assembly procedure is inappropriate for the synthesis of molecular analogues for certain "nonconventional" protein Fe/S sites that owe their stability to the protein environment. Such sites in fact may contain metastable Fe/S assemblies that, in the absence of protein constraints and given the appropriate activation energies, are likely to transform to the thermodynamically stable "conventional" clusters. Examples of sites that may contain the $[Fe_3S_4]$ nonconventional cluster cores recently have been identified in proteins such as Fd I of *Azotobacter vinelandii*,[8,9] Fd II of *Desulfovibrio gigas*,[9,10] and aconitase from beef heart.[9,11] Thus far spontaneous self-assembly reactions have not resulted in the isolation of analogue clusters that contain the Fe_3S_4 nonlinear cores, and it appears likely that such cores may be stable only within a protein environment.

The synthesis of metastable Fe/S clusters that may serve as active site analogues for NHIP with unusual properties at this stage must rely on the judicious or serendipitous choice of conditions. Such conditions should allow for the isolation of kinetic products that will have to overcome a certain activation energy barrier before they eventually transform to the thermodynamically more stable products.

In this paper we report on the synthesis and the spectroscopic and electrochemical properties of the new, metastable, $(Fe_6S_6X_6)^{3-}$ cluster series (X = Cl^-, Br^-, I^-, $p\text{-}MeC_6H_4O^-$, $p\text{-}MeC_6H_4S^-$) that contain the hitherto unknown $[Fe_6S_6]^{3+}$ cores. The single-crystal X-ray crystal structure of the $(Fe_6S_6Cl_6)^{3-}$ anion communicated earlier[12] also is reported in detail.

Experimental Section

(1) Synthesis. The chemicals in this research were used as purchased. Dimethylformamide (DMF) was stored over 4A Linde molecular sieves for 24 h and then distilled under reduced pressure at ~30 °C. Acetonitrile (CH_3CN) was distilled from calcium hydride (CaH_2) before use. Commercial grade methylene chloride (CH_2Cl_2) and diethyl ether were distilled from CaH_2. Absolute ethanol was used without any further purification. Sodium aryl mercaptides were obtained by the reaction of sodium metal with the appropriate aryl thiols in tetrahydrofuran under dinitrogen. All syntheses were carried out under a dinitrogen atmosphere in a Vacuum Atmospheres Dri-Lab glovebox. Elemental analyses, on samples dried under vacuum for 12 h, were performed by Galbraith Analytical Laboratories, Knoxville, TN.

(2) Physical Methods. Visible and ultraviolet spectra were obtained on a Cary Model 219 spectrophotometer.

Electrochemical measurements were performed with a PAR Model 173 potentiostat/galvanostat and a PAR Model 175 universal programmer. The electrochemical cell used had platinum working and auxiliary electrodes. As reference electrode a saturated calomel electrode was used. All solvents used in the electrochemical measurements were properly dried and distilled; the tetra-*n*-butylammonium perchlorate (Bu_4NClO_4) was used as the supporting electrolyte. Normal concentrations used were ~0.001 M in electroanalyte and 0.1 M in supporting electrolyte. Purified argon was used to purge the solutions prior to the electrochemical measurements. The powder diffraction diagrams were obtained by using a 114-mm diameter Debye–Scherrer-type camera with Ni-filtered Cu Kα radiation (λ = 1.5418 Å).

Mössbauer spectra were measured from 4.2 K to room temperature with a constant acceleration spectrometer. The source was 100 mCi ^{57}Co in Rh matrix and held at room temperature. EPR spectra were recorded at X-band and P-band on a Varian E-112 spectrometer and a locally constructed[13] spectrometer, respectively. Cryogenic temperatures were obtained with a helium flow system.

(3) Preparation of Compounds. Tris(tetraethylammonium) Hexachlorohexakis(μ_3-sulfido)hexaferrate(3II,3III) [$(Et_4N)_3(Fe_6S_6Cl_6)\cdot CH_3CN$] (I). A mixture of anhydrous $FeCl_2$, 1.00 g (7.87 mmol), NaSPh, 1.56 g (11.80 mmol), $Et_4NCl\cdot H_2O$, 0.70 g (3.93 mmol), and elemental sulfur, 0.50 g (15.6 mmol), was stirred at room temperature in 35 mL of CH_3CN for ca. 15 min, and the resulting brown solution was filtered to remove NaCl and unreacted sulfur. To the filtrate 120 mL of diethyl ether was added. After it stood for 8–10 h, a black microcrystalline product formed and was isolated. It was washed twice with EtOH and CH_2Cl_2 and finally with diethyl ether; yield 1.20 g, 81%. The product can be recrystallized from CH_3CN/ether mixtures.

Anal. Calcd for $Fe_6S_6Cl_6N_4C_{26}H_{63}$ (M_r = 1172): C, 26.6; H, 5.37; N, 4.78; Fe, 28.67; S, 16.38. Found: C, 26.41; H, 5.11; N, 4.80; Fe, 27.68; S, 15.02.

Tris(tetraethylammonium) Hexabromohexakis(μ_3-sulfido)hexaferrate(3II,3III) [$(Et_4N)_3(Fe_6S_6Br_6)$]. A mixture of anhydrous $FeBr_2$, 1.00 g (4.63 mmol), NaSPh, 0.91 g (6.94 mmol), Et_4NBr, 0.49 g (2.31 mmol), and elemental sulfur, 0.40 g (12.5 mmol), was stirred for ca. 5 min in 35 mL of CH_2Cl_2. The brown solution that developed was filtered and the precipitate that formed was collected and washed thoroughly with CH_2Cl_2 until the washings were colorless. This crude product is contaminated with NaBr and unreacted elemental sulfur. It was recrystallized from a CH_3CN–diethyl ether mixture. One more recrystallization from the same mixture afforded analytically pure product, 0.60 g, 57% yield.

Anal. Calcd for $Fe_6S_6Br_6N_3C_{24}H_{60}$ (M_r = 1398): C, 20.60; H, 4.29; Fe, 24.03; S, 13.73. Found: C, 19.38; H, 4.01; Fe, 23.12; S, 12.19.

Tris(tetraethylammonium) Hexaiodohexakis(μ_3-sulfido)hexaferrate(3II,3III) [$(Et_4N)_3(Fe_6S_6I_6)$]. A procedure identical with that for the bromo analogue was used. Reagents used are anhydrous FeI_2, 2.00 g (6.45 mmol), NaSPh, 1.23 g (9.67 mmol), Et_4NI, 0.83 g (3.22 mmol), or $Et_4NCl\cdot H_2O$, 0.59 g (3.22 mmol), and 0.40 g (12.5 mmol) of elemental sulfur; yield 0.90 g, 50%. The compound can be recrystallized from CH_3CN–diethyl ether mixtures.

Anal. Calcd for $Fe_6S_6I_6N_3C_{24}H_{60}$ (M_r = 1680): C, 17.14; H, 3.57; N, 2.50; Fe, 20.00. Found: C, 17.52; H, 3.82; N, 2.57; Fe, 18.86.

Tris(tetraethylammonium) Hexakis(*p*-methylphenolato)hexakis(μ_3-sulfido)hexaferrate(3II,3III) [$(Et_4N)_3(Fe_6S_6(OC_6H_4\text{-}p\text{-}Me)_6)$] (III). An amount of $(Et_4N)_3Fe_6S_6Cl_6$ (0.80 g, 0.68 mmol) was dissolved in 50 mL of CH_3CN, and to this solution solid $NaOC_6H_4\text{-}p\text{-}Me$ was added (0.60 g, 4.61 mmol). The resulting mixture was stirred for 15 min. Immediate color change to brown-red occurred upon mixing. The solution was filtered to remove NaCl, and to the filtrate 150 mL of diethyl ether was added. After the solution stood overnight, 0.80 g of pure black crystals was obtained, washed with ether, and dried in vacuo; yield 75.4%.

Anal. Calcd for $Fe_6S_6O_6N_3C_{66}H_{102}$ (MW = 1560): C, 50.77; H, 6.54; N, 2.69; Fe, 21.54. Found: C, 49.59; H, 6.04; N, 2.32; Fe, 18.69.

Tris(tetraethylammonium) Hexakis(*p*-methylphenylthiolato)hexakis(μ_3-sulfido)hexaferrate(3II,3III) [$(Et_4N)_3(Fe_6S_6(SC_6H_4\text{-}p\text{-}Me)_6)$]. An amount of $(Et_4N)_3(Fe_6S_6Cl_6)$ (0.50 g, 0.43 mmol) and $NaSC_6H_4\text{-}p\text{-}Me$ (0.38 g, 2.60 mmol) was added to 60 mL of CH_3CN and the mixture was stirred for 5 min. The mixture was filtered to remove NaCl, and to the purple filtrate 50 mL of diethyl ether were added. After the mixture stood overnight at −20 °C, a black solid formed and was isolated (0.35 g, 49% yield). The product from various preparations was contaminated with small amounts (<10%) of microcrystalline $(Et_4N)_2(Fe_4S_4(SC_6H_4\text{-}p\text{-}Me)_4)$. All attempts to crystallize the crude product were unsuccessful due to its rapid transformation to the Fe_4S_4 cubane. The electrochemical measurements, electronic spectra, Mössbauer spectra, and EPR spectra were obtained on the crude product.

Formation of $(Et_4N)_2(Fe_4S_4Cl_4)$[14a] from $(Et_4N)_3(Fe_6S_6Cl_6)$. A brown solution of 0.60 g of $(Et_4N)_3Fe_6S_6Cl_6$ in 40 mL of CH_3CN was heated up to the boiling point (81.6 °C) for ca. 10 min. The color changes to a darker brown with a purplish cast. After allowing the solution to cool to room temperature, 150 mL of diethyl ether was added. After the mixture stood for 3–4 h, 0.52 g of $(Et_4N)_2(Fe_4S_4Cl_4)$ was collected; yield 90%.

Reaction of $(Et_4N)_3(Fe_6S_6Cl_6)$ with Ph_4PCl. To a solution of $(Et_4N)_3(Fe_6S_6Cl_6)$ (0.40 g, 0.34 mmol) in 50 mL of CH_3CN, 0.80 g (2.13 mmol) of Ph_4PCl was added and the mixture was stirred for 5 min and then allowed to stand for 2 h. A slight color change was observed toward dark brown with a purplish tinge. Following filtration of the solution, 150 mL of diethyl ether was added to incipient crystallization. Upon standing for 2 h, 0.50 g of black microcrystals was obtained (83% yield). This product is identical in all respects with an authentic sample of $(Ph_4P)_2(Fe_4S_4Cl_4)$.[14]

(7) Cecconi, F.; Ghilardi, C. A.; Midollini, S. *J. Chem. Soc., Chem. Commun.* **1981**, 640.
(8) Ghosh, D.; O'Donnell, S.; Furey, W., Jr.; Robbins, A. H.; Stout, D. C. *J. Mol. Biol.* **1982**, *158*, 73–109.
(9) Beinert, H.; Thomson, A. J. *Arch. Biochem. Biophys.* **1983**, *222*, 333–361.
(10) Antonio, M. R.; Averill, B. A.; Moura, I.; Moura, J. J. G.; Orme-Johnson, W. H.; Teo, B. K.; Xavier, A. V. *J. Biol. Chem.* **1982**, *257*, 6646–6649.
(11) Beinert, H.; Emptage, M. H.; Dreyer, J. L.; Scott, R. A.; Hahn, J. E.; Hodgson, K. O.; Thomson, A. J. *Proc. Natl. Acad. Sci. U.S.A.* **1983**, *80*, 383–396.
(12) Kanatzidis, M. G.; Dunham, W. R.; Hagen, W. R.; Coucouvanis, D. *J. Chem. Soc., Chem. Commun.* **1984**, 356–358.
(13) (a) Reid, J. A. Ph.D. Thesis, The University of Michigan, 1976. (b) Stevenson, R. C. Ph.D. Thesis, The University of Michigan, 1976.

Table I. Summary of Crystal Data, Intensity Collection, Structure Solution, and Refinement

	$(Et_4N)_3(Fe_6S_6Cl_6)\cdot CH_3CN$
formula	$C_{18}H_{43}N_4Fe_6S_6Cl_6$
M_r	1172
a, Å	20.092 (5)
b, Å	17.937 (6)
c, Å	13.790 (4)
α, deg	90.00
β, deg	91.33 (2)
γ, deg	90.00
Z, V, Å^3	4, 4968
d_{calcd}, g/cm^3	1.57
d_{obsd},[a] g/cm^3	1.55
space group	$C2/c$
cryst dimens, mm	(0.40) × (0.32) × (0.38)
radiatn	Mo ($\lambda_{K\bar{\alpha}}$ = 0.71069)
abs coeff, μ, cm^{-1}	22.6
unique data	3269
data used in refinement	
$F_o^2 > 3\sigma(F_o^2)$	2604
data collecd	$h,\pm k,\pm l$, 2θ = 45, 6875
no. of variables	206
no. of atoms in asymmetric unit	50
phasing technique	direct methods
R, %[b]	4.70
R_w, %[c]	4.87

[a] Determined by flotation in a CCl_4/pentane mixture. [b] $R = \sum|\Delta F|/\sum|F_o|$. [c] $R_w = [\sum w(\Delta F)^2/\sum w(F_o)^2]^{1/2}$.

A similar result is obtained if $Et_4NCl\cdot H_2O$ is used instead of Ph_4PCl.

(4) X-ray Diffraction Measurements. Collection of Data. A single crystal resembling an approximate cuboctahedron was mounted in a capillary tube and used for data collection. Details concerning crystal characteristics and X-ray diffraction methodology are shown in Table I. Intensity data were collected for one-half of the reciprocal lattice sphere on a Nicolet P3/F four-circle diffractometer. A detailed description of the instrument and the data acquisition procedures have been given[15] previously.

Reduction of Data. The raw data were reduced to net intensities, estimated standard deviations were calculated on the basis of counting statistics, Lorentz–polarization corrections were applied, and equivalent reflections were averaged. The estimated standard deviation of the structure factor was taken as the larger of that derived from counting statistics and that derived from the scatter of multiple measurements.

The least-squares program used minimizes $\sum w(\Delta|F|)^2$. The weighting function used throughout the refinement of the structure gives zero weight to those reflections with $F^2 \leq 3\sigma(F^2)$ and $w = 1/\sigma^2(F)$ to all others $[\sigma^2(F^2) = (0.06F^2)^2 + \sigma^2(F^2)$ (from counting statistics)].[16]

The scattering factors of the neutral non-hydrogen atoms were taken from the tables of Doyle and Turner,[17] and real and imaginary dispersion corrections[18] were applied to all of them. The spherical hydrogen scattering factor tables of Stewart, Davidson, and Simpson[19] were used.

Determination of the Structure of $(Et_4N)_3(Fe_6S_6Cl_6)\cdot CH_3CN$ (I). The structure of I was solved by direct methods using the SOLV routine of the SHELXTL[20] package of crystallographic programs. The anion is required by symmetry to reside on a crystallographic inversion center. The Fe_3S_3 unique fragment of the Fe_6S_6 core was initially located, and the rest of the non-hydrogen atoms were found from successive Fourier difference electron density maps. There are two crystallographically independent Et_4N^+ cations, one of which occupies a general position in the lattice while the other is required to reside on a crystallographic 2-fold axis. The latter was found to have positionally disordered carbon atoms with approximate 50% occupancies. Isotropic refinement of all the atoms resulted in an R value of 0.11. The refinement then continued assigning anisotropic temperature factors to all nondisordered atoms. After two cycles of refinement, a CH_3CN molecule of solvation was located along the crystallographic 2-fold axis. This molecule was included in the refinement and was assigned isotropic temperature factors. At this stage the hydrogen atom positions were calculated (C–H 0.95 Å) and included in the structure factor calculation but were not refined. The final R value was 0.047, and the weighted R_w was 0.049. During the last cycle of refinement, all parameter shifts were less than 10% of their esd.

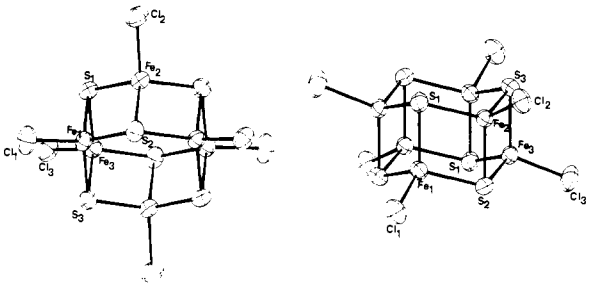

Figure 1. Structure and labeling of the $(Fe_6S_6Cl_6)^{3-}$ anion (two views). Thermal ellipsoids are drawn by ORTEP (Johnson, C. K., ORNL-3794, Oak Ridge National Laboratory, Oak Ridge, TN, 1965) and represent the 50% probability surfaces.

Crystallographic Results. The final atomic positional and thermal parameters for non-hydrogen atoms of the $(Et_4N)_3(Fe_6S_6Cl_6)$ with standard deviations derived from the inverse matrix of the least-squares refinement are compiled in Table II. Intramolecular distances and angles for the anion are given in Table III. The atom labeling scheme of the anion is shown in Figure 1.

Results and Discussion

Synthesis. In a previous publication we have reported[14b] on the reaction between $FeCl_2$, NaSPh, Ph_4PCl, and RSSSR (R = benzyl, C_7H_7) in CH_3CN that affords in excellent yield the $(Ph_4P)_2(Fe_4S_4Cl_4)$ cluster according to the stoichiometry:

$$4FeCl_2 + 6NaSPh + 2Ph_4Cl + 4RSSSR \rightarrow (Ph_4P)_2(Fe_4S_4Cl_4) + 4RSSR + 3PhSSPh + 6NaCl \quad (1)$$

The Bu_4N^+ salt also can be obtained readily by the same general reaction, and as a source of sulfide ions elemental sulfur can be used in place of RSSSR. The above reaction (eq 1) follows a different course when Et_4N^+ is used as a counterion and all other conditions are kept the same. In the presence of Et_4N^+ the new cluster $(Et_4N)_3(Fe_6S_6Cl_6)$ complex is obtained in 80% yield (eq 2).

$$6FeCl_2 + 9NaSPh + 3Et_4NCl + 6S \rightarrow (Et_4N)_3(Fe_6S_6Cl_6) + 4.5PhSSPh + 9NaCl \quad (2)$$

A slight modification of this procedure allows for the synthesis of the analogous $(Et_4N)_3Fe_6S_6X_6$ (X = Br, I) clusters. Specifically, the reaction is carried out in CH_2Cl_2 where the desired products are insoluble and precipitate out of the reaction mixture as they form.

The $(Fe_6S_6X_6)^{3-}$ clusters are homologous to the $(Fe_4S_4X_4)^{2-}$ "cubanes" and represent the second entry to a class of clusters with the general formulation $((Fe_2S_2X_2)^{1-})_n$.

The apparent cation dependence in the synthesis of the $(Fe_6S_6Cl_6)^{3-}$ cluster is somewhat surprising in view of the fact that the Et_4N^+ salt of the $(Fe_4S_4Cl_4)^{2-}$ is a known stable compound.[14] In our synthetic studies we have observed that the synthesis of the $(Fe_6S_6Cl_6)^{3-}$ hexanuclear cluster is accomplished successfully only when the Et_4N^+ cation is present in solution from the beginning of the reaction. If the reaction is allowed to proceed in the absence of the Et_4N^+ cation, which is added after the reaction should have gone to completion, the only product that can be isolated in high yield is the $(Et_4N)_2(Fe_4S_4Cl_4)$ cluster. The Et_4N^+ cation appears to be the only counterion thus far that is capable of stabilizing the $(Fe_6S_6Cl_6)^{3-}$ cluster in the synthetic procedure outlined previously and allows for its isolation in both high quality and quantity. We were unable to obtain entirely satisfactory elemental analysis for the crystalline $(Et_4N)_3(Fe_6S_6Cl_6)$. However, the X-ray powder pattern of this material was identical with the pattern calculated on the basis of the single-crystal data and conclusively indicates that both the single crystal and the bulk

(14) (a) Wong, G. B.; Bobrik, M. A.; Holm, R. H. *Inorg. Chem.* **1978**, *17*, 528. (b) Coucouvanis, D.; Kanatzidis, M.; Simhon, E.; Baenziger, N. C. *J. Am. Chem. Soc.* **1982**, *104*, 1874.
(15) Kanatzidis, M. G.; Coucouvanis, D. *Inorg. Chem.* **1984**, *23*, 403.
(16) Grant, D. F.; Killean, R. C. G.; Lawrence, J. L. *Acta Crystallogr., Sect. B* **1969**, *B25*, 374.
(17) Doyle, P. A.; Turner, P. S. *Acta Crystallogr., Sect. A* **1968**, *A24*, 390.
(18) Cromer, D. T.; Liberman, D. *J. Chem. Phys.* **1970**, *53*, 1891.
(19) Stewart, R. F.; Davidson, E. R.; Simpson, W. T. *J. Chem. Phys.* **1965**, *42*, 3175.
(20) SHELXTL package of Crystallographic Programs, Nicolet XRD Corporation, Fremont, CA.

Table II. Positional and Thermal Parameters[a] and Standard Deviation[b] for the Anion in $(Et_3N)_3(Fe_6S_6Cl_6)\cdot CH_3CN$

atom	x	y	x	atom	x	y	x
Fe(1)	0.2843 (1)	0.7232 (1)	0.3419 (1)	C(6)	0.2796 (5)	0.5926 (5)	−0.0599 (8)
Fe(2)	0.3652 (1)	0.7258 (1)	0.5073 (1)	C(7)	0.1538 (6)	0.4657 (6)	−0.1412 (9)
Fe(3)	0.2669 (1)	0.6432 (1)	0.5934 (1)	C(8)	0.0278 (6)	0.6013 (7)	−0.0800 (10)
S(1)	0.3421 (1)	0.8224 (1)	0.4056 (2)	N(2)	0.0	0.0422 (5)	0.2500
S(2)	0.3081 (1)	0.6270 (1)	0.4429 (1)	C(9)	−0.0663 (6)	0.0417 (6)	0.0876 (8)
S(3)	0.3245 (1)	0.7418 (1)	0.6580 (1)	C(10)	0.0	0.1871 (9)	0.2500
Cl(1)	0.3113 (1)	0.6922 (1)	0.1917 (1)	C(11)	0.022 (16)	0.0419 (19)	0.1454 (23)
Cl(2)	0.4745 (1)	0.7064 (1)	0.5184 (2)	C(12)	0.0406 (9)	0.1138 (10)	0.2117 (13)
Cl(3)	0.2772 (1)	0.5364 (1)	0.6737 (1)	C(13)	0.0650 (9)	0.0342 (10)	0.2947 (13)
N(1)	0.1523 (3)	0.5908 (4)	−0.0560 (5)	C(14)	−0.0526 (10)	−0.0184 (11)	0.2838 (15)
C(1)	0.1523 (5)	0.6232 (6)	0.0477 (7)	C(15)	−0.0260 (11)	−0.0964 (13)	0.2576 (19)
C(2)	0.2139 (4)	0.6166 (5)	−0.1065 (7)	C(16)	−0.0131 (39)	0.0512 (38)	0.1020 (56)
C(3)	0.1503 (5)	0.5065 (5)	−0.0508 (8)	CS(1)	0.5000	0.2076 (11)	0.2500
C(4)	0.0940 (5)	0.6211 (6)	−0.1154 (8)	CS(2)	0.5000	0.1389 (20)	0.2500
C(5)	0.1527 (6)	0.7068 (6)	0.0569 (8)	CS(3)	0.4847 (14)	0.0727 (13)	0.2936 (19)

atom	U_{11}	U_{22}	U_{33}	U_{23}	U_{13}	U_{12}
Fe(1)	0.0360 (7)	0.0352 (7)	0.0386 (7)	−0.0033 (5)	−0.0023 (5)	0.0018 (5)
Fe(2)	0.0315 (7)	0.0415 (7)	0.0435 (7)	−0.0059 (6)	−0.0038 (5)	0.0026 (5)
Fe(3)	0.0403 (7)	0.0337 (7)	0.0419 (7)	−0.0022 (5)	−0.0022 (5)	0.0040 (5)
S(1)	0.0351 (12)	0.0387 (12)	0.0546 (14)	−0.0028 (10)	−0.0022 (10)	−0.0044 (9)
S(2)	0.0462 (13)	0.0322 (11)	0.0416 (12)	−0.0035 (9)	−0.0020 (10)	0.0027 (9)
S(3)	0.0349 (12)	0.0488 (13)	0.0439 (12)	−0.0102 (10)	−0.0054 (10)	0.0022 (10)
Cl(1)	0.0647 (15)	0.0549 (14)	0.0409 (12)	−0.0/43 (10)	0.0016 (11)	0.0142 (11)
Cl(2)	0.0346 (12)	0.0914 (19)	0.0667 (16)	−0.0170 (14)	−0.0071 (11)	0.0115 (12)
Cl(3)	0.0743 (17)	0.0466 (14)	0.0555 (14)	0.0101 (11)	0.0026 (12)	0.0153 (12)
N(1)	0.0494 (46)	0.0487 (45)	0.0570 (46)	0.0099 (36)	−0.0062 (37)	0.0078 (35)
C(1)	0.0643 (72)	0.0962 (87)	0.0497 (58)	0.0021 (56)	0.0045 (50)	0.0109 (59)
C(2)	0.0594 (58)	0.0427 (52)	0.0636 (60)	0.0096 (45)	0.0077 (50)	0.0042 (44)
C(3)	0.0580 (68)	0.0437 (61)	0.1150 (94)	0.0201 (62)	−0.0057 (62)	−0.0004 (48)
C(4)	0.0662 (63)	0.0580 (64)	0.0829 (73)	−0.0007 (54)	−0.0255 (58)	0.0078 (52)
C(5)	0.0847 (79)	0.0896 (90)	0.0786 (77)	−0.0273 (65)	−0.0025 (62)	0.0081 (65)
C(6)	0.0590 (57)	0.0519 (59)	0.0886 (71)	−0.0053 (54)	0.0055 (56)	−0.0022 (49)
C(7)	0.0847 (82)	0.0483 (66)	0.1230 (98)	−0.0120 (67)	−0.0181 (71)	−0.0035 (57)
C(8)	0.0665 (70)	0.0913 (92)	0.1531 (24)	−0.0203 (87)	−0.0329 (81)	0.0217 (69)
N(2)	0.0466 (64)	0.0512 (64)	0.0446 (59)	0.0	−0.0060 (48)	0.0
C(9)	0.0130 (26)	0.0	0.0	0.0	0.0	0.0
C(10)	0.0794 (45)	0.0	0.0	0.0	0.0	0.0
C(11)	0.0819 (88)	0.0	0.0	0.0	0.0	0.0
C(12)	0.0526 (46)	0.0	0.0	0.0	0.0	0.0
C(13)	0.0595 (50)	0.0	0.0	0.0	0.0	0.0
C(14)	0.0672 (55)	0.0	0.0	0.0	0.0	0.0
C(15)	0.0905 (76)	0.0	0.0	0.0	0.0	0.0
C(16)	0.5102 (15)	0.0	0.0	0.0	0.0	0.0
CS(1)	0.0953 (53)	0.0	0.0	0.0	0.0	0.0
CS(2)	0.1820 (12)	0.0	0.0	0.0	0.0	0.0
CS(3)	0.2370 (23)	0.0	0.0	0.0	0.0	0.0

[a] Thermal parameters are in units of square Angstroms. The temperature factor has the form $T = -\sum(1/4U(IJ)H(I) - H(J)\text{ASTAR}(I)\text{ASTAR}(J))$. H is the Miller index, ASTAR is the reciprocal cell length, and I and J are cycled 1-3. [b] Calculated standard deviations are indicated in parentheses.

material are chemically identical species.

It would appear that the successful isolation of the $(Et_4N)_3(Fe_6S_6Cl_6)$ salt is not due to counterion lattice stabilization effects but rather to effective and specific ion association in the early stages of the reaction which may result in the stabilization of the appropriate kinetic intermediate. The metastable nature of the $(Fe_6S_6Cl_6)^{3-}$ anion is evident in the facile quantitative transformation of this cluster to $(Fe_4S_4Cl_4)^{2-}$ by mild heating in CH_3CN solution (Figure 1, eq 3).

$$2(Fe_6S_6Cl_6)^{3-} \rightarrow 3(Fe_4S_4Cl_4)^{2-} \quad (3)$$

This transformation is accelerated in coordinating solvents such as DMF, *N*-methylpyrrolidone (NMP), and dimethyl sulfoxide (Me_2SO) and is rather slow in CH_3NO_2.

A possible mechanism for this transformation, which also is catalyzed by halide ions, may involve ligand (X^- or L) assisted dissociation of the cluster into $(Fe_2S_2Cl_4)^{3-}$ intermediates and subsequent dimerization (Scheme I). The proposed scheme is consistent with (a) the known rapid dimerization[21] of the $(Fe_2S_2Cl_4)^{3-}$ species to $(Fe_4S_4Cl_4)^{2-}$ and (b) the nearly quantitative

Scheme I

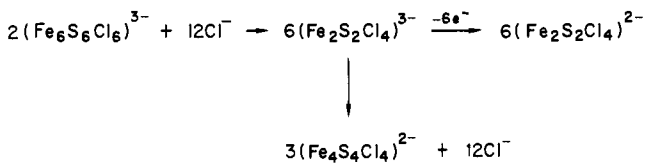

conversion of the $(Fe_6S_6Cl_6)^{3-}$ anion to the $(Fe_2S_2Cl_4)^{2-}$ dimer in the presence of Cl^- ions and an oxidizing agent (Cu^{+2}) in CH_3CN solution.

A parallel reaction that occurs between $(Fe_6S_6Cl_6)^{3-}$ and nucleophiles is ligand substitution (eq 4). When this reaction is

$$(Et_4N)_3(Fe_6S_6Cl_6) + 6X^- \rightarrow (Et_4N)_3(Fe_6S_6X_6) + 6Cl^- \quad (4)$$

carried out in CH_3CN solution using NaX ($X = I^-$, PhS^-, PhO^-) the rapid precipitation of NaCl allows for the isolation of the $(Fe_6S_6X_6)^{3-}$ salts with minimum contamination by the $(Fe_4S_4X_4)^{2-}$ homologues. The $(Fe_6S_6(SPh)_6)^{3-}$ cluster is exceedingly unstable in solution and transforms to the $(Fe_4S_4(SPh)_4)^{2-}$ within minutes at ambient temperature (Figure 2). By far the greatest stabilization of the $[Fe_6S_6]^{3+}$ cores is affected by phenoxide ligands and single crystals of the $(Et_4N)_3(Fe_6S_6(OC_6H_4\text{-}p\text{-}Me)_6)$ salt are

(21) Cambray, J.; Lane, R. W.; Wedd, A. G.; Johnson, R. W.; Holm, R. H. *Inorg. Chem.* **1972**, *16*, 2565.

Table III. Selected Distances (Å) and Angles in the Anion[a] of the Et_4N^+ Salt of $Fe_6S_6Cl_6^{3-}$

		Distances	
Fe(1)-Fe(2)	2.771 (1)	Fe(1)···Fe(2)	3.778 (1)
Fe(2)-Fe(3)	2.760 (1)	Fe(2)···Fe(3)	3.806 (1)
Fe(1)-Fe(3)	2.764 (1)	Fe(1)···Fe(3)	3.785 (1)
mean[b]	2.765 (3)	mean	3.790 (8)
Fe(1)-S(1)	2.290 (2)	Fe(1)-Cl(1)	2.223 (2)
Fe(2)-S(2)	2.278 (2)	Fe(2)-Cl(2)	2.226 (2)
Fe(3)-S(3)	2.284 (2)	Fe(3)-Cl(3)	2.222 (2)
mean	2.284 (3)	mean	2.224 (2)
Fe(1)-S(2)	2.263 (2)	S(1)-S(2)	3.610 (3)
Fe(1)-S(3)	2.274 (2)	S(2)-S(3)	3.617 (3)
Fe(2)-S(1)	2.270 (2)	S(3)-S(1)	3.628 (3)
Fe(2)-S(3)	2.278 (2)	mean	3.618 (5)
Fe(3)-S(1)	2.275 (2)	S(1)···S(3)	3.789 (3)
Fe(3)-S(2)	2.272 (2)	S(2)···S(3)	3.794 (3)
mean	2.272 (2)	S(1)···S(2)	3.819 (3)
mean of 9	2.268 (3)	mean	3.801 (9)
		Angles	
S(1)-Fe(1)-S(3)	113.5 (1)	Fe(2)-S(1)-Fe(3)	112.8 (1)
S(1)-Fe(2)-S(3)	113.2 (1)	Fe(1)-S(2)-Fe(3)	112.9 (1)
S(2)-Fe(3)-S(1)	114.3 (1)	Fe(2)-S(3)-Fe(1)	113.8 (1)
mean	113.7 (3)	mean	113.2 (3)
S(2)-Fe(1)-S(1)	104.9 (1)	Fe(1)-S(1)-Fe(2)	74.8 (1)
S(3)-Fe(1)-S(1)	105.2 (1)	Fe(1)-S(1)-Fe(3)	74.5 (1)
S(2)-Fe(2)-S(1)	105.1 (1)	Fe(1)-S(2)-Fe(2)	75.2 (1)
S(2)-Fe(2)-S(3)	105.5 (1)	Fe(2)-S(2)-Fe(3)	74.7 (1)
S(2)-Fe(3)-S(3)	105.2 (1)	Fe(1)-S(3)-Fe(3)	74.7 (1)
S(1)-Fe(3)-S(3)	105.0 (1)	Fe(2)-S(3)-Fe(3)	74.7 (1)
mean	105.1 (2)	mean	74.7 (1)
mean of 9	108 (2)	Fe(1)-Fe(3)-Fe(2)	87.1 (1)
Cl(1)-Fe(1)-S(1)	114.8 (1)	Fe(1)-Fe(2)-Fe(3)	86.1 (1)
Cl(2)-Fe(2)-S(2)	113.1 (1)	Fe(3)-Fe(1)-Fe(2)	86.2 (2)
Cl(3)-Fe(3)-S(3)	115.7 (1)	mean	86.5 (3)
mean	114.5 (7)		
Cl(1)-Fe(1)-S(2)	109.3 (1)	Fe(2)-Fe(1)-Fe(3)	59.9 (1)
Cl(1)-Fe(1)-S(3)	109.0 (1)	Fe(1)-Fe(2)-Fe(3)	59.7 (1)
Cl(2)-Fe(2)-S(1)	110.4 (1)	Fe(2)-Fe(3)-Fe(1)	60.4 (1)
Cl(2)-Fe(2)-S(3)	109.5 (1)	mean	60.0 (2)
Cl(3)-Fe(3)-S(2)	108.3 (1)		
Cl(3)-Fe(3)-S(1)	108.0 (1)		
mean	109.1 (3)		
mean of 9	111 (1)		

[a] For the cations in $[Et_4N]_2Fe_6S_6Cl_6$, the N-C bonds are within the range of 1.500 (10)-1.541 (11) Å with a mean value of 1.516 (18) Å for cation of N(1), and 1.443 (29)-1.610 (18) Å with a mean value of 1.52 (9) Å for the disordered Et_4N^+ of N(2). The six C(*i*)-N(1)-C(*j*) angles are found between 105.9 (7)° and 111.4 (7)° with a mean value of 109 (2)°. For the cations the scatter estimate was obtained as follows: $S = [\sum_{i=1}^{N}(X_i - \bar{x})^2/N - 1]^{1/2}$ where x_i is the value of an individual bond or angle and $\bar{x}$ is the mean value for the N equivalent bond lengths or angles. [b] The standard deviation from the mean, σ, is reported: $\sigma = [\sum_{i=1}^{N}(X_i - \bar{x})^2/N(N-1)]^{1/2}$.

obtained readily by the diffusion of ether to CH_3CN solutions of this compound.[22]

Description of the Structure. The unit cell of $(Et_4N)_3(Fe_6S_6Cl_6)$ contains well-separated Et_4N^+ cations and $(Fe_6S_6Cl_6)^{3-}$ anions. The former are found in the crystal in two crystallographically independent groups. One-third of the cations reside on 2-fold axes and are disordered while the other two-thirds occupy general positions in the lattice. Their structures are unexceptional and will not be considered further.

The anion (Figure 1) is situated on a crystallographic center of symmetry at 3/4, 1/4, 0 and contains the $[Fe_6S_6]^{3+}$ unit as a distorted hexagonal prism with iron and sulfur atoms occupying alternate vertices. The Fe_6 and S_6 interpenetrating units, which form the core in the anion, have trigonally compressed octahedral structures and so does the Cl_6 unit. The latter consists of the Cl^- terminal ligands that complete the tetrahedral coordination sphere around each of the six metal centers.

(22) Crystal data for $(Et_4N)_3Fe_6S_6(OC_6H_4\text{-}p\text{-}Me)_6$: Crystal system monoclinic P, cell dimensions a = 13.35 (1) Å, b = 20.10 (2) Å, c = 14.45 (3) Å, β = 97.0 (1)°, V = 3847, Z = 2, d_{obsd} = 1.36 g/cm³, d_{calcd} = 1.35 g/cm³.

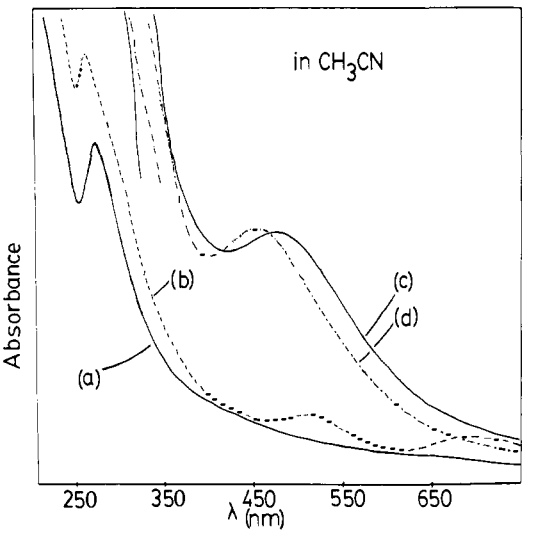

Figure 2. Cluster transformations in CH_3CN solution. (a) $(Fe_6S_6Cl_6)^{3-}$; (b) $(Fe_4S_4Cl_4)^{2-}$, obtained by heating solution (a) to 60 °C for 5 min; (c) $(Fe_6S_6(SPh)_6)^{3-}$, obtained immediately following the addition of 6 equiv of PhS^- to solution (a) at ambient temperature; (d) $(Fe_4S_4(SPh)_4)^{2-}$, obtained from solution c, after standing for 10 min at ambient temperature.

Table IV. Intramolecular Bond Distances (Å) and Angles (deg) in the $(Fe_6S_6Cl_6)^{3-}$, $(Fe_4S_4Cl_4)^{2-}$, and $(Fe_2S_2Cl_4)^{2-}$ Anions

anions	$Fe_6S_6Cl_6^{3-}$	$Fe_4S_4Cl_4^{2-a}$	$Fe_2S_2Cl_4^{2-b}$
Fe–Fe	2.765 (3)	2.766 (5)	2.716 (1)
Fe···Fe	3.790 (8)		
Fe–S	2.276 (3)	2.295 (3)	2.200 (1)
Fe–Cl	2.223 (2)	2.216 (2)	2.251 (1)
Fe–S–Fe[d]	74.7 (2)	74.5 (2)	76.2 (1)
Fe–S–Fe[c]	113.2 (3)		
S–Fe–S[d]	105.1 (2)	103.5 (3)	103.8 (1)
S–Fe–S[c]	113.7 (3)		
Cl–Fe–S	111 (1)	115 (1)	112.0 (3)
Fe–Fe–Fe[e]	86.5 (3)		
Fe–Fe–Fe[c]	60.0 (2)	60.0	

[a] Reference 14a. [b] Reference 44. [c] Values within the Fe_3S_3 "cyclohexane" fragment. [d] Values within the Fe_2S_2 "rhombic" fragment. [e] Fe–Fe–Fe angles within two adjacent Fe_2S_2 units.

The structure of the $[Fe_6S_6]^{3+}$ core can be analyzed in terms of two identical cyclohexane-chair Fe_3S_3 units eclipsed relative to each other and oriented in a way that the sulfide ions from one unit serve as ligands for the iron atoms in the other. The dihedral angles, S(1)Fe(3)S(2)/S(1)S(2)Fe(1)Fe(2) and Fe(1)S(3)′Fe(2)′/S(1)S(2)Fe(1)Fe(2)′ within the Fe_3S_3 cyclohexane chair are 136.2° and 136.0°, respectively. The prism can be described also in terms of three Fe_2S_2 planar rhombic units fused so as to yield the hexagonal prismatic arrangement. The three independent dihedral angles between the rhombic sides of the hexagonal prism are 120.8°, 119.6° and 119.6°, respectively.

Two types of Fe–Fe distances and Fe–S–Fe angles are present in the anion (Table III). Within the hexagonal bases of the prism these values (Fe_b–Fe_b, 3.790 (8) Å; Fe_b–S–Fe_b, 113.2 (3)°) resemble the values reported[8] for the (Fe_3S_3) unit in the structure of *A. vinelandii* ferredoxin I (Fe–Fe, 4.00 Å, range 3.94 (10)–4.05 (10) Å; Fe–S–Fe, 117°, range 113 (5)–121 (5)°). A significant difference in the two structures exists in the geometry of the Fe_3S_3 fragments, which in the *A. vinelandii* ferredoxin is nearly planar.

The Fe_s–Fe_s distances and Fe_s–S–Fe_s angles within the planar Fe_2S_2 rhombic side units at 2.765 (6) Å and 74.7 (2)°, respectively (Table III), are quite similar to corresponding values in the $(Fe_2S_2L_4)^{2-}$ and $(Fe_4S_4L_4)^{2-}$ clusters (Table IV). The Fe–S distances in the Fe_6S_6 core are found within a narrow range and cannot be divided into sets that are indicative of any systematic

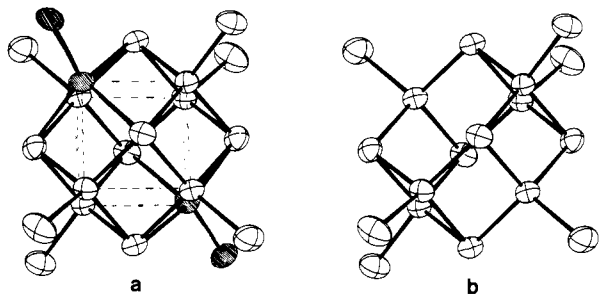

Figure 3. (a) The structure of the hypothetical $(M_8S_6Cl_8)^{4-}$ cluster obtained by the addition of two ML units (shaded atoms) to the $(M_6S_6Cl_6)^{3-}$ prismane cluster. (b) The structure of the $(Fe_6S_6Cl_6)^{3-}$ cluster in identical orientation to the $M_6S_6Cl_6$ unshaded fragment in (a).

Table V. Structural Parameters of $(Fe_6S_6Cl_6)^{3-}$, $(Co_8S_6(SPh)_8)^{4-}$, Co_9S_8, and $(Fe, Ni)_8S_8Ag$

dist, Å, angles, deg	$Fe_6S_6Cl_6^{3-}$	$Co_8S_6(SPh)_8^{4-}$ [a]	Co_9S_8 [b]	$(Fe,Ni)_8S_8Ag$ [c]
M–M	2.765 (6)	2.662 (16)		2.676 (2)
M···M	3.790 (8)	3.758 (19)		3.663 (2)
M–S	2.276 (5)	2.230 (10)		2.264 (2)
M–L	2.224 (2)	2.241 (9)		2.243 (2)
M–S–M [d]	74.8 (2)	73.3		72.29 (5)
M–S–M [e]	113.2 (3)	115.0		113.00 (3)
S–M–S	113.7			111.26 (3)
S–M–S	105.2	106.5	111.4	107.63 (3)
M–M–M [d]	86.5	90.1	90	86.4
M–M–M [e]	60.0		60.0	60.0

[a] Reference 27. [b] Reference 24. [c] Reference 26. [d] Within the M_2S_2 planar units. [e] Within the M_3S_3 cyclohexane fragments.

deviations from the idealized D_{3d} symmetry. The Fe–S bonds connecting the two Fe_3S_3 units are slightly longer than the others; however, the difference (0.022 Å) is within 3σ and is not statistically significant. The mean value of all Fe–S bonds (2.276 (8) Å) is similar to the corresponding value in the homologous $(Fe_4S_4Cl_4)^{2-}$ (2.283 (5) Å; Table IV).

A prismatic M_6S_6 core similar to Fe_6S_6 also has been found in the centrosymmetric metal cages of the heterometallic silver tetrathiometallate complexes $(R_3P)_4Ag_4(MS_4)_2$ (M = Mo, W).[23]

The Fe_6S_6 core in the present structure is very nearly an exact fragment of the larger metal sulfide cages found in the natural mineral pentlandites such as Co_9S_8,[24] $(Ni,Fe)_9S_8$,[25] or $(Fe,Ni)_8AgS_8$.[26] These minerals contain recognizable M_8S_6 units which consist of a cube of metal atoms inscribed into an octahedron of μ_4 bridging sulfide ligands. This arrangement generates a rhombic dodecahedral $[M_8(\mu_4\text{-}S)_6]^{4+}$ core unit with planar M_2S_2 faces and idealized O_h symmetry (Figure 3a). An identical M_8S_6 unit is found in the recently reported[27] $(Co_8S_6(SPh)_8)^{4-}$ cluster which contains discrete $[Co_8S_6]$ cores ligated by PhS^- terminal ligands.

The generation of a M_6S_6 fragment of D_3d symmetry from a pentlandite type M_8S_6 cage can be accomplished easily if two diagonally disposed M atoms are removed from the corners of the M_8 cube in the pentlandite structure (Figure 3b). As a consequence of such a change, the quadruply bridging sulfides in M_8S_6 all are transformed to triply bridging ligands in the M_6S_6 "product" and the M–S–M angles are partitioned into two (6 + 12) sets with values of ~113° and ~73°. The extent of the topological relationship between the M_8S_6 units in the pentlandites and the Fe_6S_6 unit in the present structure is apparent in a comparison of corresponding core dimensions (Table V).

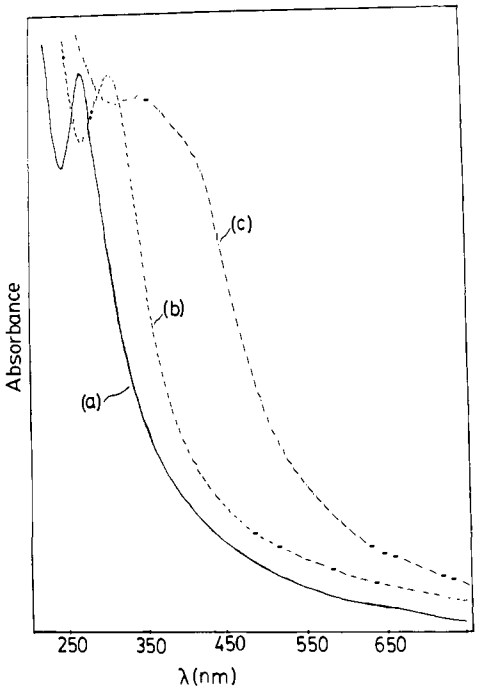

Figure 4. Electronic spectra of the $(Fe_6S_6X_6)^{3-}$ clusters ((a) X = Cl^-, (b) X = Br^-, (c) X = I^-) in CH_3CN solution.

Table VI. Electronic Spectra[a] of the $(Fe_6S_6X_6)^{3-}$ Series (X = Cl, Br, I) and $(Fe_6S_6(XC_6H_4\text{-}p\text{-}Me)_6)^{3-}$ (X = S, O)

compd[a]	λ_{max}, nm	ϵ, M^{-1} cm^{-1}
$(Fe_6S_6Cl_6)^{3-}$	270	33 880
$(Fe_6S_6Br_6)^{3-}$	306	27 990
$(Fe_6S_6I_6)^{3-}$	350	26 585
	402 (sh)	~23 000
$(Fe_6S_6(SC_6H_4\text{-}p\text{-}Me)_6)^{3-}$	480	21 330
	260	63 600
$(Fe_6S_6(OC_6H_4\text{-}p\text{-}Me)_6)^{3-}$	427	19 718
	272	42 363

[a] Obtained in 10^{-4} M CH_3CN solutions.

Recently, the structure of another Fe_6S_6 center was determined in the $(Fe_6S_6I_6)^{2-}$ cluster.[28] The oxidation level in the latter is one electron lower than the oxidation level in the $[Fe_6S_6]^{3+}$ core reported herein. The mean Fe–S and Fe–Fe distances in the $[Fe_6S_6]^{4+}$ core at 2.257 (5) and 2.741 (3) Å, respectively, are slightly shorter than those found in the $[Fe_6S_6]^{3+}$ core. A meaningful assessment of the structural differences between the two different oxidation levels, based on the results of a structure determination of the $(Fe_6S_6Cl_6)^{2-}$ cluster, has been published.[29]

Electronic Spectra. The electronic spectra of the $(Fe_6S_6X_6)^{3-}$ series (X = Cl, Br, I) show (Table VI, Figure 4) a featureless gradual absorption from 650 to ~350 nm and only one well-defined absorption maximum in the UV region. The latter is halide ligand dependent and becomes broader and shifts to lower energies in the order: I < Br < Cl. This trend is similar to the one observed in the spectra of the $(Fe_4S_4X_4)^{2-}$ series and previously attributed[14a] to X → core charge-transfer excitations. The electronic spectra of the $(Fe_6S_6(XC_6H_4\text{-}p\text{-}Me)_6)^{3-}$ (X = S, O) clusters resemble very much the spectra of the corresponding cubanes[30] and show intense absorptions in the visible region of the spectrum around 480 and 426 nm for X = S and O, respectively. Similar absorptions in the Fe_4S_4 homologues have been assigned[30] previously to X → core charge-transfer transitions.

(23) (a) Müller, A.; Diemann, E.; Jostes, R.; Bögge, H. *Angew. Chem., Int. Ed. Engl.* **1981**, *20*, 934. (b) Stalick, J. K.; Siedle, A. R.; Mighell, A. D.; Hubbard, C. R. *J. Am. Chem. Soc.* **1979**, *101*, 2908.
(24) (a) Geller, S. *Acta Crystallogr.* **1962**, *15*, 1195. (b) Rajamani, V.; Prewitt, C. T. *Can. Mineral.* **1975**, *13*, 75.
(25) Rajamani, V.; Reweitt, C. T. *Can. Mineral.* **1973**, *12*, 178.
(26) Hall, S. R.; Stewart, J. M. *Can. Mineral.* **1973**, *12*, 169.
(27) Christou, G.; Hagen, K. S.; Holm, R. H. *J. Am. Chem. Soc.* **1982**, *104*, 1744.
(28) Saak, W.; Henkel, G.; Pohl, S. *Angew. Chem., Int. Ed. Engl.* **1984**, *23*.
(29) Coucouvanis, D.; Kanatzidis, M. G.; Lester, R.; Hagen, W. R.; Dunham, W. R. *J. Am. Chem. Soc.* **1984**, *106*, 7998.
(30) DePamphilis, B. V.; Averill, B. A.; Herskovitz, T.; Que, L.; Holm, R. H. *J. Am. Chem. Soc.* **1974**, *96*, 4159.

Table VII. Cyclic Voltammetric Data for the $(Fe_6S_6L_6)^{3-}$ Clusters[a,b]

	oxidn 2-/3-				Reductn 3-/4-			
	E_{pa}	$E_{1/2}$	ΔE, mV	i_{pc}/i_{pa}	E_{pc}	$E_{1/2}$	ΔE, mV	i_{pa}/i_{pc}
				in CH_3CN				
$Fe_6S_6Cl_6^{3-}$	+0.303			0.0	-0.820	-0.750	141	0.77
$Fe_6S_6(OC_6H_4$-*p*-$Me)_6^{3-}$	-0.110			0.0	*c*			
$Fe_6S_6(SC_6H_4$-*p*-$Me)_6^{3-}$	-0.153	-0.222	138	0.96	-1.096	-1.036	115	0.30
				in CH_2Cl_2				
$Fe_6S_6Cl_6^{3-}$	+0.301	+0.243	116	1.0	-0.824	-0.704	139	0.77
$Fe_6S_6(OC_6H_4$-*p*-$Me)_6^{3-}$	-0.102	-0.194	184	0.96	*c*			
$Fe_6S_6(SC_6H_4$-*p*-$Me)_6^{3-}$	-0.084	-0.165	163	0.98	-1.096			0.10

[a] For all measurements the scan rate was 200 mV/s. [b] The supporting electrolyte was 0.1 M $(Ph_4P)ClO_4$. [c] Not well-defined wave.

Electrochemical Measurements. The electrochemical behavior of the $(Fe_6S_6L_6)^{3-}$ "prismanes" with L = Cl, SC_6H_4-*p*-Me, or OC_6H_4-*p*-Me was studied by cyclic voltammetry in CH_3CN and CH_2Cl_2 and the results are summarized in Table VII.

The $(Fe_6S_6Cl_6)^{3-}$ complex in CH_3CN solution exhibits a well-defined wave for the 3-/4- reduction at -0.820 V (at 200 mV/s). The separation between the anodic and cathodic waves, ΔE (141 mV), and a i_{pa}/i_{pc} value of 0.73 indicate a quasi-reversible electron-transfer process and a chemically unstable reduction product. At positive potentials (+0.303 V at 200 mV/s) an irreversible $1e^-$ oxidation process is observed and underscores the instability of the $(Fe_6S_6Cl_6)^{2-}$ in CH_3CN. Cyclic voltammetric measurements in CH_2Cl_2 solution show quasi-reversible reduction at -0.824 V (200 mV/s) with i_{pa}/i_{pc} ratios of ~0.7 and reversible oxidation at 0.301 V. The apparent stability of the oxidation product in CH_2Cl_2 makes this solvent the obvious choice for the successful chemical oxidation of $(Fe_6S_6Cl_6)^{3-}$. The chemical oxidation of the latter, in CH_2Cl_2 with $((C_5H_4)_2Fe)^+$ as the oxidant, proceeds cleanly and affords in high yield the $(Fe_6S_6Cl_6)^{2-}$ dianion.[29]

When excess Cl^- ion is added to either CH_3CN or CH_2Cl_2 solutions of the prismane trianion, the voltammetric measurements show the presence of only $(Fe_4S_4Cl_4)^{2-}$ and illustrate the destabilizing effects of the chloride ions.

The cyclic voltammetric behavior of $(Fe_6S_6(OC_6H_4$-*p*-$Me)_6)^{3-}$ in CH_3CN is similar to that of the chloro analogue. No well-defined reduction occurs and two irreversible oxidation waves are observed at -0.110 and +0.400 V. Severe electrode absorption effects presented a problem, however, and well-defined cyclic voltammograms could be obtained only when the working electrode was cleaned before each scan. The behavior in CH_2Cl_2 solution is much cleaner and one oxidation is found at -0.102 V. This process involves one electron and is also attributed to the 2-/3- couple. By electrochemical standards, the cyclic voltammetric wave is not reversible (ΔE > 60 mV, increase of ΔE with scan rate) but this could be due to the high residual resistance of the CH_2Cl_2 solvent, part of which remained uncompensated during the experiment. The i_{pc}/i_{pa} ratios, however, approach unity and this implies effective chemical reversibility.

The $(Fe_6S_6(SC_6H_4$-*p*-$Me)_6)^{3-}$ cluster in CH_2Cl_2 solution also undergoes reversible oxidation and displays a voltammetric wave at -0.084 V with quite similar characteristics. Surprisingly, this cluster shows reversible oxidation at -0.153 V in CH_3CN solution as well as with ΔE = 138 mV and $i_{pc}/i_{pa} \sim 1$.

Mössbauer Spectra. The hyperfine parameters in the Mössbauer spectra of the $(Et_4N)_3(Fe_6S_6L_6)$ compounds (in the solid at 125 K and zero applied field, vs. Fe) are shown in Table VIII. These values are compared to representative members of the $(Fe_4S_4L_4)^{2-}$ series. The spectra consist of single, sharp quadrupole doublets for each of the entries and clearly indicate that all six of the iron atoms in the $(Fe_6S_6)^{3+}$ are equivalent as a result of complete charge delocalization throughout the core. A similar charge delocalization also is evident in the spectra of the $(Fe_4S_4L_4)^{2-}$ clusters which consist of single quadrupole doublets as well.

Table VIII. Isomer Shifts[a] and Quadrupole Splittings of $[Fe_6S_6(L)_6]^{3-}$ Clusters (L = Cl, Br, I, SC_6H_4-*p*-Me, OC_6H_4-*p*-Me) and $[Fe_4S_4(L')_4]^{2-}$ Clusters (L' = Cl, SPh, OPh)

cluster	*T*, K	IS, mm/s	ΔE_Q, mm/s
$(Et_4N)_3[Fe_6S_6Cl_6]$	125	0.495 (1)[b]	1.085 (1)
$(Et_4N)_3[Fe_6S_6Br_6]$	125	0.493 (1)	1.132 (1)
$(Et_4N)_3[Fe_6S_6I_6]$	125	0.485 (1)	1.128 (1)
$(Et_4N)_3[Fe_6S_6(OC_6H_4$-*p*-$Me)_6]$	125	0.476 (1)	1.016 (1)
$(Et_4N)_3[Fe_6S_6(SC_6H_4$-*p*-$Me)_6]$	125	0.440 (1)	1.043 (1)
$(Ph_4P)_2[Fe_4S_4Cl_4]$[c]	77	0.49 (1)	0.67 (1)
$(Ph_4P)_2[Fe_4S_4(SPh)_4]$[c]	77	0.43 (1)	0.93 (1)
$(Et_4N)_2[Fe_4S_4(OPh)_4]$[d]	4.2	0.50 (1)	1.21 (1)

[a] With respect to Fe metal at room temperature. [b] Estimated uncertainty from the computer fitting. [c] From ref 32. [d] From ref 33.

An inspection of the data (Table VIII) shows that the trends in the isomer shift (IS) values as a function of terminal ligand, L, in the prismane complexes parallel similar trends in the corresponding "cubane" complexes and show the isomer shift increasing in the order Cl ~ Br > I > OPh > SPh. The similar quadrupole splitting, ΔE_q, and IS values in the spectra of the corresponding homologous Fe_4S_4 and Fe_6S_6 clusters and the sensitivity of these values to temperature preclude the use of Mössbauer spectra as diagnostic criteria for differentiating between the two types of clusters.

The fundamental electronic difference between the $[Fe_4S_4]^{2+}$ and $[Fe_6S_6]^{3+}$ cores lies in the description of their ground states. The former possesses a diamagnetic (S = 0) while the latter a paramagnetic ($S = {}^1/_2$) ground state (vide infra). This difference may allow for cluster-type identification from Mössbauer spectra obtained in weak applied magnetic fields. By contrast to the low-temperature spectra of the $(Fe_4S_4L_4)^{2-}$ clusters that are not affected by weak magnetic fields,[31] the spectra of the $(Fe_6S_6L_6)^{3-}$ clusters are perturbed by the application of weak (500 G) magnetic fields.

The Mössbauer spectra of the $(Fe_6S_6Cl_6)^{3-}$ cluster in frozen acetonitrile solution are shown in Figure 5. The zero applied field spectrum (Figure 5a) was fitted by a single quadrupole doublet (solid line) with IS and ΔE_Q values of 0.496 (1) and 1.063 (1) mm/s, respectively (T = 125 K). These parameters together with the asymmetry parameter η (0.41) were used for the successful simulation of the spectra obtained in the presence of an applied magnetic field (Figure 5c; H_{app} = 56.6 kG; T = 125 K). The high quality of the fit demonstrates the similarity of the six iron sites in the $(Fe_6S_6Cl_6)^{3-}$ cluster.

The low- (H_{app} = 0.5 kG) and high- (H_{app} = 59 kG) field spectra at 4.2 K are shown in Figure 5, parts b and d, respectively. The low-field spectrum (Figure 5b) shows that part of the quadrupole doublet observed in the zero field spectrum (Figure 5a) is still present. This observation suggests that the spin-lattice relaxation time for the $(Fe_6S_6Cl_6)^{3-}$ cluster is short even at 4.2 K.

In the high-field spectra (Figure 5d), there is no apparent evidence for this doublet, and Boltzmann factors result in population of only the ground electronic Zeeman state regardless of

(31) Debrunner, P. G.; Münck, E.; Que, L.; Schulz, C. E. In "Iron-Sulfur Proteins"; Lovenberg, W., Ed.; Academic Press: New York, 1977; Vol. III, Chapter 10 and references therein.
(32) Kanatzidis, M. G.; Baenziger, N. C.; Coucouvanis, D.; Simopoulos, A.; Kostikas, A. *J. Am. Chem. Soc.*, submitted for publication.
(33) Cleland, W. E.; Holtman, D. A.; Sabat, M.; Ibers, J. A.; DeFotis, G. C.; Averill, B. A. *J. Am. Chem. Soc.* **1983**, *105*, 6021.

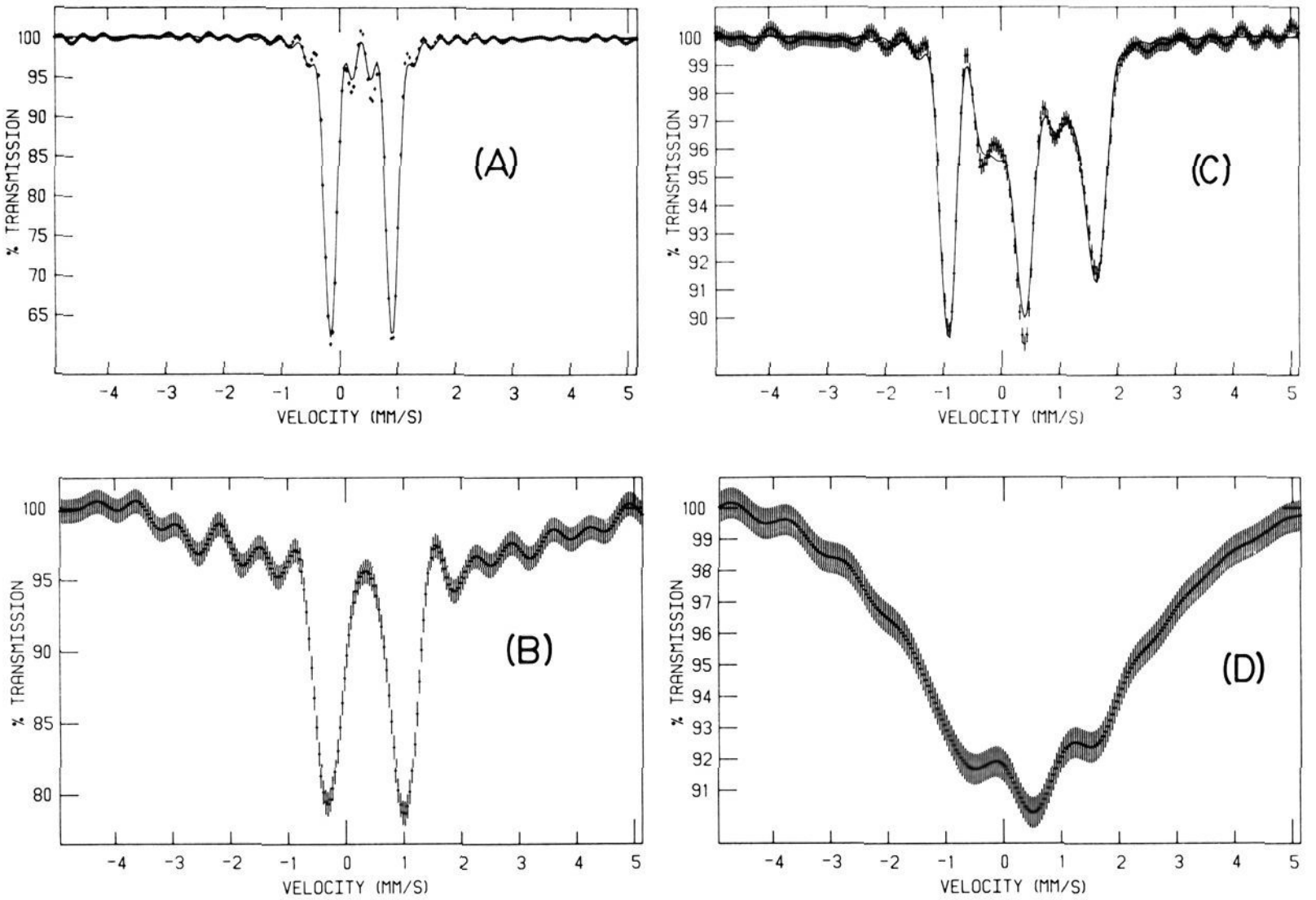

Figure 5. Mössbauer spectra of $(Et_4N)_3Fe_6S_6Cl_6$ in frozen CH_3CN solution at (A) T = 125 K, H = 0; (B) T = 4.5 K, H = 0.5 kG; (C) T = 125 K, H = 56.6 kG; (D) T = 4.3 K, $H \approx 59$ kG. In all cases the applied magnetic field was parallel to the γ-rays. The spectra were deconvoluted for the source line shape [—] but not exponentiated to form absorption spectra.

the relaxation rate. It appears therefore that all six iron atoms are part of the spin system, and that they all have nonzero a tensors. At temperatures well below 4.2 K, the fast relaxation process that "smears" the nuclear interactions may be slowed down. Under such conditions electron nuclear double-resonance (ENDOR) experiments should allow for a determination of the a tensor projections.

Electron Paramagnetic Resonance (EPR) Spectra and Magnetic Susceptibility Measurements. The EPR spectra of the $(Fe_6S_6L_6)^{3-}$ clusters (L = Cl^-, p-$MeC_6H_4S^-$, p-$MeC_6H_4O^-$) were examined in frozen CH_3CN solutions at temperatures between 6 and 19 K. Representative spectra at ~8 K are shown in Figure 6.

The spectra of $(Et_4N)_3(Fe_6S_6Cl_6)$ and $(Et_4N)_3(Fe_6S_6(SC_6H_4$-$p$-$Me)_6)$ were simulated with the following parameters:[34] $g_x = 2.038$, $g_y = 1.71$, and $g_z = 1.2$ for the former and $g_x = 2.029$, $g_y = 1.79$, and $g_z = 1.3$ for the latter. Using the simulated g values in a quantitation[35] based on the area of the low-field half of the low-field peak vs. the second integral of a copper standard signal, we find 1.08 $S = {}^1/_2$ systems per $(Et_4N)_3(Fe_6S_6(L)_6)$ cluster. The EPR spectra are indicative of very efficient spin–lattice relaxation as evidenced by the absence of any microwave power saturation at low temperature and by extensive signal broadening at temperatures above ~9 K. The integrated intensity of the low-field half of the low-field line closely follows Curie's law over the temperature range from 6.6 to 19 K. The clusters are not completely magnetically isolated even in dilute solution. The simulation requires a "residual broadening" that amounts to about 10% of the total width along the axis corresponding to $g = 2.038$. This broadening from intercluster dipolar interactions becomes apparent when the EPR signal of the $(Fe_6S_6Cl_6)^{3-}$ cluster is measured as a function of concentration (Figure 7). Dilution to a concentration of 0.04 mM actually leads to the resolution of the g_y line.

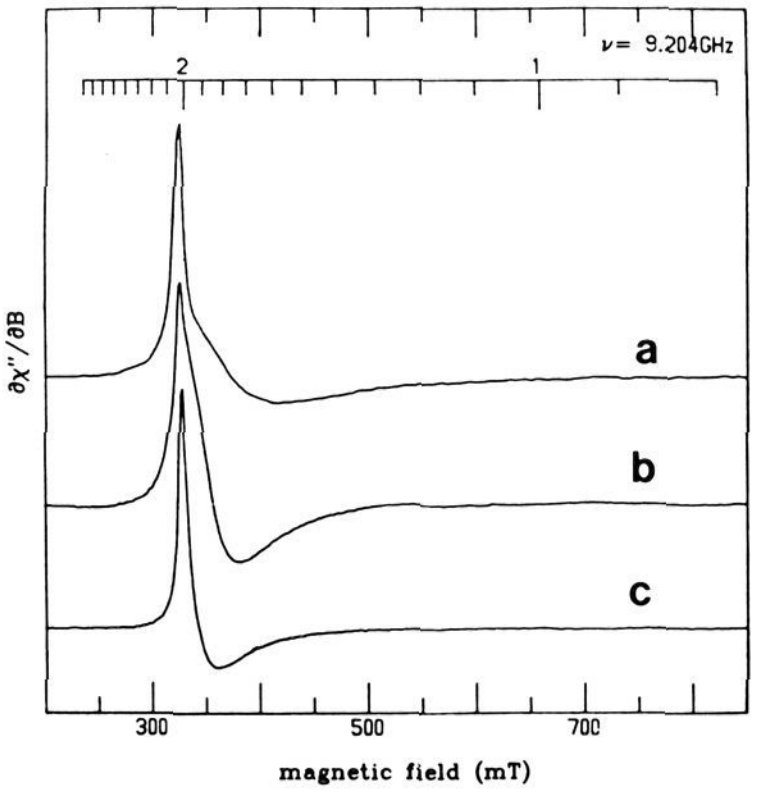

Figure 6. EPR spectra of the $[Fe_6S_6Cl_6]^{3-}$ clusters in CH_3CN at 8–9 K. (a) $(Et_4N)_3Fe_6S_6Cl_6$, 0.7 mM; (b) $(Et_4N)_3Fe_6S_6(SC_6H_4$-p-$Me)_6$, 0.4 mM; (c) $(Et_4N)_3Fe_6S_6(OC_6H_4$-p-$Me)_6$, 1.35 mM. Experimental conditions: Microwave frequency 9204 MHz, microwave power 200 mW, modulation amplitude 1.25 mT, modulation frequency 100 kHz.

However, at these low concentrations, a significant amount of the cluster is affected by an unidentified contaminant in the solvent. As a result the signal does not account quantitatively for the expected concentration of the $(Fe_6S_6Cl_6)^{3-}$ cluster, and the spectrum shows a $g = 4.3$ line arising from high-spin Fe(III) (not shown in Figure 7). At higher concentrations, resolution is increasingly lost until a featureless spectrum is obtained.

Except for an order of magnitude larger field span, the overall shape of the EPR spectra resembles the shape of the signal ob-

(34) (a) Hagen, W. R.; Hearshen, D. O.; Sands, R. H.; Dunham, W. R. *J. Magn. Reson.*, in press. (b) Hagen, W. R.; Hearshen, D. O.; Harding, L. J.; Dunham, W. R. *J. Magn. Reson.*, in press.

(35) Aasa, R.; Vänngard, T. *J. Magn. Reson.* **1975**, *19*, 308–315.

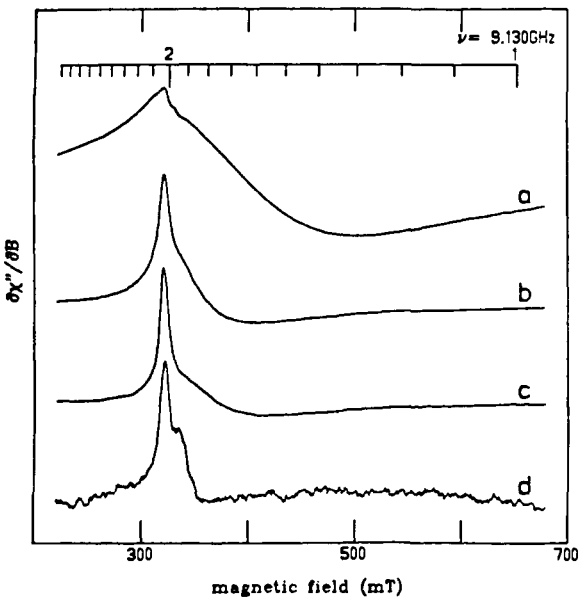

Figure 7. Concentration dependence of the X-band line shape of $(Et_4N)_3Fe_6S_6Cl_6$ in the solid and in CH_3CN at 8.0–9.1 K. Trace (a) solid crystals, trace (b) 10 mM frozen solution, trace (c), 0.7 mM frozen solution, trace (d) 0.04 mM frozen solution. Experimental conditions were as in Figure 6.

tained for the oxidized 3Fe center in *D. gigas* Fd II[36] and ferredoxins from *M. barkeri*,[37] *T. thermophilus*,[38] and *A. vinelandii*.[39]

The molar magnetic susceptibility of the $(Et_4N)_3(Fe_6S_6Cl_6)$ cluster was measured[40] from 1.5 to 290 K and is consistent with a $S = {}^1/_2$ ground state. The details of the magnetic behavior of the $(Fe_6S_6X_6)^{3-}$ cluster will be published elsewhere.[41]

Summary and Conclusions

The $(Fe_6S_6L_6)^{3-}$ metastable clusters are new members in the general series of Fe/S clusters that contain the $[Fe_2S_2]_n^{n+}$ cores. The latter (n = 1, 2) are common structural units in the active sites of various Fe/S proteins.[4] In recent years new, unconventional Fe/S core structures such as $[Fe_3S_3]^{3+}$ and $[Fe_3S_4]^{+}$ have been found[8] or proposed[9] to exist in a number of Fe/S proteins. To date the $[Fe_2S_2]_3^{3+}$ prismatic core has not been considered as a possible structural unit in any of the known Fe/S proteins.

The spectroscopic, electrochemical, and magnetic properties of the $[Fe_2S_2]_3^{3+}$ cores in the synthetic $(Fe_6S_6L_6)^{3-}$ clusters now introduce a new set of criteria for the consideration and possible identification of similar cores in Fe/S proteins with unusual characteristics.

Of the spectroscopic properties, the electronic and zero-field Mössbauer spectra of the $[Fe_6S_6]^{3+}$ cores are very similar to those of the $[Fe_4S_4]^{2+}$ cores, particularly when the terminal ligands are RS^- or RO^- (Table VI). As such they are not expected to be useful diagnostic indicators for the possible identification of the Fe_6S_6 cores. The EPR (Figure 6) and magnetic Mössbauer spectra (Figure 5), however, are unique and should be indicative of the presence of the ($S = {}^1/_2$) $[Fe_6S_6]^{3+}$ cores.

The increased stability of the $[Fe_6S_6]^{3+}$ core with phenoxide terminal ligands suggests that a full compliment of six cysteinyl ligands may not be a requirement for the attachment of a Fe_6S_6 core to a protein "backbone". Consequently a number of cysteinyl residues less than six should not automatically exclude the possible presence of a Fe_6S_6 unit.

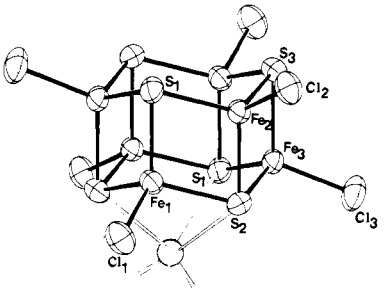

Figure 8. Hypothetical interaction of the $[Fe_6S_6L_6]^{3-}$ clusters with a MoL_3 unit and generation of a Fe_6MoS_6 core.

The electrochemical results show that the $[Fe_6S_6]^{2+/3+}$ redox couple functions at a more positive potential (Table VII) than the $[Fe_4S_4]^{2+/3+}$ couple (for the same terminal ligands). The redox potential, therefore, represents an additional functional constraint that must be considered together with other criteria in site identification arguments.

The core extrusion reactions that have been used effectively[42,43] for the quantitative determination of cluster content in the conventional NHIP rely on the thermodynamic stability of the Fe_4S_4 cores outside the protein. Such core extrusion reactions clearly are not expected to be reliable for Fe/S site-type identification or quantitation in proteins that, by virtue of their spectroscopic characteristics, do not belong unequivocally to a recognized general class and may contain *metastable* Fe/S cores other than Fe_4S_4. The metastable nature of the $[Fe_6S_6]^{3+}$ cores clearly indicates that core extrusion reactions are not likely to reveal the presence of such species. The facile transformation of the latter to the $[Fe_4S_4]^{2+}$, more stable cores may indeed lead to erroneous conclusions for core extrusion experiments that involve Fe/S proteins that contain $[Fe_6S_6]^{3+}$ cores.

Finally, the Fe_6S_6 prismane cage represents a new addition to the multiiron Fe/S cages that may be considered as possible structural candidates for the Fe component fragment in the Fe–Mo–S site of nitrogenase. A Mo substituted Fe_7MoS_6 "pentlandite" core has been suggested previously[27] as a possible structural unit for the Fe–Mo–S site in nitrogenase. A similar unit can be constructed by the addition of a MoL_x appendix on top of the S_3 triangular array in one of the Fe_3S_3 bases of the Fe_6S_6 prismane. The monocapped $MoFe_6S_6$ prism that results from this addition is shown in Figure 8. The synthesis and characterization of heterometallic cages of this type presently are under study in our laboratory.

Acknowledgment. This research was supported by a grant from the National Institutes of Health (GM-26671). X-ray equipment used in this research was obtained in part by a grant (CHE.8109065) from the National Science Foundation.

Registry No. I, 94499-90-8; III, 94499-96-4; $(Et_4N)_3(Fe_6S_6Br_6)$, 94499-92-0; $(Et_4N)_3(Fe_6S_6I_6)$, 94499-94-2; $(Et_4N)_3(Fe_6S_6(SC_6H_4$-$p$-$Me)_6)$, 94499-98-6; $(Et_4N)_2(Fe_4S_4Cl_4)$, 62758-02-5; $(Ph_4P)_2(Fe_4S_4Cl_4)$, 80765-12-4; $Fe_6S_6Cl_6^{2-}$, 93530-53-1; $Fe_6S_6(OC_6H_4$-p-$Me)_6^{2-}$, 94499-99-7; $Fe_6S_6(SC_6H_4$-p-$Me)_6^{2-}$, 94500-00-2; $Fe_6S_6Cl_6^{4-}$, 94500-01-3; Fe_6S_6-$(SC_6H_4$-p-$Me)_6^{4-}$, 94517-74-5.

Supplementary Material Available: Tables of structure factors and positional and thermal parameters for I (14 pages). Ordering information is given on any current masthead page.

(36) Huynh, B. H.; Moura, J. J. G.; Moura, I.; Kent, T. A.; LeGall, J.; Xavier, A. V.; Münck, E. *J. Biol. Chem.* **1980**, *255*, 3242–3244.
(37) Moura, I.; Moura, J. J. G.; Huynh, B. H.; Santos, H.; LeGall, J.; Xavier, A. V. *Eur. J. Biochem.* **1982**, *126*, 95–98.
(38) Hille, R.; Yoshida, T.; Tarr, G. E.; Williams, C. H.; Ludwig, M. L.; Fee, J. A.; Kent, T. A.; Huynh, B. H.; Münck, E. *J. Biol. Chem.* **1983**, *258*, 13008–13013.
(39) Sweeney, W. V.; Rabinowitz, J. C.; Yoch, D. C. *J. Biol. Chem.* **1975**, *250*, 7842–7847.
(40) The magnetic susceptibility data were obtained on a SQUID magnetometer at Michigan State University, East Lansing, MI, in Professor J. Dye's laboratories.
(41) Dunham, W. R.; Hagen, W. R.; Coucouvanis, D.; Kanatzidis, M. G., manuscript in preparation.
(42) Averill, B. A.; Bale, J. R.; Orme-Johnson, W. H. *J. Am. Chem. Soc.* **1978**, *100*, 3034.
(43) Kurtz, D. M.; Holm, R. H.; Ruzickz, F. J.; Beinert, H.; Coles, C. J.; Singer, T. P. *J. Biol. Chem.* **1979**, *254*, 4967.
(44) Bobrik, M. A.; Hodgson, K. O.; Holm, R. H. *Inorg. Chem.* **1977**, *16*, 1851.